Frontiers of Information Technology & Electronic Engineering
www.jzus.zju.edu.cn; engineering.cae.cn; www.springerlink.com
ISSN 2095-9184 (print); ISSN 2095-9230 (online)
E-mail: jzus@zju.edu.cn

# Prior information based channel estimation for millimeter-wave massive MIMO vehicular communications in 5G and beyond*

Zhao YI[†1], Weixia ZOU[†‡1,2], Xuebin SUN[1]

[1]*MOE Key Laboratory of Universal Wireless Communications, Beijing University of Posts and Telecommunications, Beijing 100876, China*

[2]*State Key Laboratory of Millimeter Waves, Southeast University, Nanjing 210096, China*

[†]E-mail: yz17tx@bupt.edu.cn; zwx0218@bupt.edu.cn

Received Sept. 30, 2020; Revision accepted Jan. 21, 2021; Crosschecked May 1, 2021

**Abstract:** Millimeter wave (mmWave) has been claimed as the viable solution for high-bandwidth vehicular communications in 5G and beyond. To realize applications in future vehicular communications, it is important to take a robust mmWave vehicular network into consideration. However, one challenge in such a network is that mmWave should provide an ultra-fast and high-rate data exchange among vehicles or vehicle-to-infrastructure (V2I). Moreover, traditional real-time channel estimation strategies are unavailable because vehicle mobility leads to a fast variation mmWave channel. To overcome these issues, a channel estimation approach for mmWave V2I communications is proposed in this paper. Specifically, by considering a fast-moving vehicle secnario, a corresponding mathematical model for a fast time-varying channel is first established. Then, the temporal variation rule between the base station and each mobile user and the determined direction-of-arrival are used to predict the time-varying channel prior information (PI). Finally, by exploiting the PI and the characteristics of the channel, the time-varying channel is estimated. The simulation results show that the scheme in this paper outperforms traditional ones in both normalized mean square error and sum-rate performance in the mmWave time-varying vehicular system.

**Key words:** Massive multiple-input multiple-output; Millimeter wave; Channel estimation; Vehicular communication; Time-varying

https://doi.org/10.1631/FITEE.2000515 **CLC number:** TN928

## 1 Introduction

To realize reliable communications in fast-mobility scenarios, such as on high-speed vehicles, the future millimeter-wave (mmWave) massive multiple-input multiple-output (MIMO) wireless communication (the emerging 5G and beyond) networks of connected vehicles are desired. However, mobile network operators face significant growth in data traffic demand, and this trend is expected to accelerate over the next decade with the rise of the Internet-of-Things (IoT) (Brady et al., 2013; Heath et al., 2016; Rappaport et al., 2017). One of the main candidates to address high data traffic demand is mmWave wireless communications (Gu and Leshem, 2012; Brady et al., 2013; Sayeed and Brady, 2013; Rappaport et al., 2017; Shaham et al., 2018), which use mmWave technology to provide unprecedented spectrum and multi-gigabit per second (Gb/s) data rates for mobile devices in fast variation channels.

Exploiting the high data rate of mmWave

‡ Corresponding author

* Project supported by the National Natural Science Foundation of China (No. 61971063)

ORCID: Zhao YI, https://orcid.org/0000-0001-7131-4232; Weixia ZOU, https://orcid.org/0000-0002-1452-9787; Xuebin SUN, https://orcid.org/0000-0002-7508-4945

paves the way for exciting applications, such as mmWave cellular systems and vehicle-to-infrastructure (V2I) and vehicle-to-vehicle (V2V) communications. Moreover, due to that a base station (BS) is usually much taller than vehicles, the existence of line-of-sight (LoS) paths in vehicular communications makes high-bandwidth technology more suitable (Brady et al., 2013).

Although mmWave techniques can provide high performance required by various applications, vehicular communications still face many challenges, because more and more vehicles are connected to the IoT and this makes these networks more complicated. For example, vehicular networks operate under more severe conditions than common cellular networks due to the time-varying channel, which significantly reduces coherence time (Brady et al., 2013). Moreover, it is particularly difficult to achieve high beamforming, because the beamforming process must be completed in an extremely short time. On the other hand, mmWave relies heavily on finding directional links with high beamforming gains to compensate for existing defects, which requires frequent and accurate channel estimation (Sayeed and Brady, 2013). In addition, the complexity of channel estimation and the number of required feedback bits increase with large antenna arrays (Shaham et al., 2018). Furthermore, the high mobility feature of vehicles increases the frequency of channel estimation even further.

To cope with these shortcomings, numerous works have been conducted on the applications of mmWave massive MIMO time-varying channels (Kabaoglu, 2009; Fernandez et al., 2010; Bourdoux et al., 2011; Gu et al., 2014; Awad et al., 2015; Choi et al., 2016; Gao et al., 2017a; Ma et al., 2018; Wu et al., 2019). Although the complexity of transceivers is reduced by hybrid analog/digital structures, the high cost of hardware prevents the transceivers from exploiting one dedicated radio frequency (RF) chain for each equipped antenna (Awad et al., 2015; Ma et al., 2018; Wu et al., 2019; Brighente et al., 2020), and hybrid beamforming schemes require more pilot overhead for fast time-varying channels (Garcia et al., 2016; Kong et al., 2017). Although many channel tracking schemes have been researched in the applications of mmWave V2I communication (Bourdoux et al., 2011; Gu et al., 2014; Awad et al., 2015; Gao et al., 2017a; Mehrabi et al., 2020), however, those schemes are suitable only for the terahertz frequency band and cannot be applied to fast time-varying mmWave channels. Apart from that, works studied by Awad et al. (2015) and Zhang et al. (2016) have modeled slowly time-varying channels in adjacent time slots using a one-order Markov process, and the classical Kalman filter was used to track the time-varying channels. However, those schemes are adopted only at microwave frequencies, and the mmWave beamspace channels with special sparse structure cannot be modeled by the one-order Markov process. Additionally, support detection based beamspace channel estimation schemes were designed by Gao et al. (2017b) and Shen et al. (2019). Gao et al. (2017a) and Bourdoux et al. (2011) proposed channel estimation and tracking algorithms for time-varying beamspace channels. Unfortunately, existing channel estimation techniques are designed mainly for point-to-point, real-time, or slowly time-varying scenarios, and the pilot overhead is still high especially for multiuser scenarios.

Importantly, most of those works (Zhou et al., 1999; Zhang et al., 2016; Palacios et al., 2017) further enhance the estimation accuracy for vehicular networks by assuming point-to-point, slowly time-varying, or non-mmWave frequency band communication. However, those schemes are unrealistic in a dynamic environment since user mobility leads to a fast variation channel. To the best of our knowledge, mmWave channel estimation has not been deeply investigated in V2I communication scenarios, where the BS simultaneously communicates with multiple fast-moving users.

To fill this gap, we propose a novel prior information (PI) based channel estimation scheme for mmWave massive MIMO time-varying vehicle systems in an open highway scenario, which can effectively estimate the LoS path in the V2I communication scenario. Specifically, by considering the fast-moving vehicle scenario, the mathematical model of the fast time-varying channel is first established. Then, a temporal variation rule of the physical direction, i.e., the direction-of-arrival (DOA), between the BS and each mobile user is derived, and the DOA in the previous time slot is combined with the temporal variation law to estimate the DOA in the following time slot. Then, based on the estimated DOA and the special sparse structure of the time-varying beamspace channel, the support of the

channel, i.e., the PI, is detected, and the beams are selected based on the PI. Finally, the corresponding nonzero elements of the channels are estimated using the least squares (LS) algorithm, and the complete time-varying channel is estimated. Simulation results show that our proposed scheme offers better estimation accuracy for the fast-mobility channel scenario than that of the conventional support detection (SD) based scheme, which makes it attractive for mmWave time-varying vehicular communication.

Our main contributions are summarized as follows:

1. We propose a novel PI-based channel estimation scheme for the fast time-varying mmWave massive MIMO vehicular communication system, which significantly reduces the duration of channel estimation and pilot overhead, making it a viable algorithm for V2I communication scenarios.

2. The conventional spatial domain is transformed into an angular domain by discrete lens array (DLA), which effectively reduces the number of required RF chains and the dimension of the MIMO system. Moreover, based on the principle that the actual space direction is approximately equal to the predefined one, the time-varying physical direction can be determined and further refined. It can adaptively adjust the residual caused by the moving direction and speed. Thus, our method is suitable for the nonlinear mobile user model with a time-varying speed.

3. To achieve the same accuracy, the proposed method in this study needs much lower pilot overhead and signal-to-noise ratio (SNR) than the conventional scheme. Our method can accurately estimate the LoS paths between the BS and multiple fast-moving users in the V2I communication scenario, which makes it attractive for fast time-varying mmWave vehicular communication systems.

Notations used in this paper are as follows: Throughout this paper, vectors and matrices are represented by boldfaced lower-case and upper-case letters (e.g., $\boldsymbol{a}$ and $\boldsymbol{A}$), respectively. All vectors are defined as column vectors. Variables and constants are denoted in lower-case and upper-case letters (e.g., $a$ and $A$), respectively. $\boldsymbol{A}^{\mathrm{T}}$, $\boldsymbol{A}^{\mathrm{H}}$, $\boldsymbol{A}^{-1}$, and $\|\boldsymbol{A}\|$ represent the transpose, conjugate transpose, inverse, and Frobenius norm of $\boldsymbol{A}$, respectively. $|a|$ denotes the amplitude of $a$. $\boldsymbol{0}_{N\times M}$ denotes a zero matrix of size $N\times M$. $\mathcal{CN}(u,\boldsymbol{R})$ is a complex Gaussian distribution with mean $u$ and covariance matrix $\boldsymbol{R}$. $\boldsymbol{I}_N\in\mathbb{C}^{N\times N}$ denotes an $N\times N$ identity matrix. $\lceil a\rceil$ denotes the smallest integer no smaller than $a$. $\mathbb{E}[X]$ denotes the expectation of random $X$. In addition, we summarize the key notations in Table 1.

**Table 1 Description of key symbols**

| Symbol | Description |
|---|---|
| $d_k(t)$ | Communication distance between the BS and the $k^{\mathrm{th}}$ mobile user in time slot $t$ |
| $\theta_k^l$ | Physical direction of the $l^{\mathrm{th}}$ path of the $k^{\mathrm{th}}$ user |
| $\widetilde{\theta}_k(t)$ | Predicted physical direction of the $k^{\mathrm{th}}$ mobile user in time slot $t$ |
| $\overline{\theta}_k(t)$ | Time-varying physical direction of the $k^{\mathrm{th}}$ mobile user in time slot $t$ |
| $\overline{\psi}_n$ | Spatial direction predefined by discrete lens array (DLA) |
| $\psi_k^l$ | Spatial direction corresponding to the angle of arrival of the $l^{\mathrm{th}}$ component at the $k^{\mathrm{th}}$ user |
| $\psi_k(t)$ | Spatial direction corresponding to the angle of arrival of the $k^{\mathrm{th}}$ user in time slot $t$ |
| $\mathcal{I}(N)$ | Index set |
| $\boldsymbol{a}(\psi_k^l)$ | Array response vector corresponding to the $l^{\mathrm{th}}$ path of the $k^{\mathrm{th}}$ moving user in time slot $t$ |
| $\boldsymbol{U}$ | Spatial discrete Fourier transform matrix |
| $\widetilde{\boldsymbol{h}}_k$ | Beamspace channel of the $k^{\mathrm{th}}$ user |
| $\widetilde{\boldsymbol{h}}_k(t)$ | Time-varying beamspace channel of the $k^{\mathrm{th}}$ user in time slot $t$ |
| $\widetilde{\boldsymbol{h}}_k^{\mathrm{e}}(t)$ | Time-varying estimated channel of the $k^{\mathrm{th}}$ user in time slot $t$ |
| $\boldsymbol{H}_b$ | Beamspace channel with dimension $b$ predefined by DLA |
| $\widetilde{\boldsymbol{H}}_b$ | Effective channel matrix with dimension $b$ after beam selection |
| $\boldsymbol{F}_b$ | Digital precoding matrix with dimension $b$ predefining by DLA |
| $\widetilde{\boldsymbol{F}}_b$ | Digital precoding matrix with dimension $b$ after beam selection |
| $v_k$, $\alpha_k$ | Motion speed and motion direction of the $k^{\mathrm{th}}$ user, respectively |
| $\boldsymbol{f}_k(t)$ | Motion state vector of the $k^{\mathrm{th}}$ user in time slot $t$ |
| $\boldsymbol{G}^{\pm N}(\boldsymbol{x})$ | Function of $\boldsymbol{x}$ when used recursively $N$ times |
| $\widetilde{n}_k^*$ | Position of the strongest element of the time-varying channel of the $k^{\mathrm{th}}$ user |
| $\widetilde{n}_k^*(t)$ | Position of the strongest element of the time-varying channel of the $k^{\mathrm{th}}$ user in time slot $t$ |

## 2 System model

In this section, we present a model for mmWave fast time-varying vehicular communication systems. First, we explain the overall structure of the mmWave V2I communication system including the transmission scheme, physical schematics, and the transmission characteristics of the scenario. Then, the channel acquisition model is analyzed.

### 2.1 Analysis of the structure of the mmWave V2I communication system

We consider mmWave vehicular communication in a highway scenario as shown in Fig. 1. The BS is stationary while the vehicles are moving on an open highway, where there are few mountains and blockages around mobile users. The BS communicates with multiple vehicles at a short distance simultaneously. Since the BS is much taller than the vehicles, it is very likely that LoS communication is available in V2I scenarios.

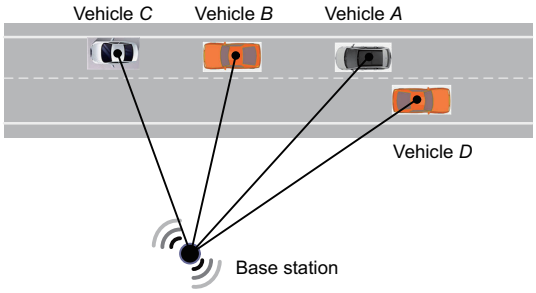


**Fig. 1 An mmWave vehicle-to-infrastructure (V2I) fast vehicular communication system model**

For mmWave fast time-varying channels in an outdoor environment, the number of dominant scatters is limited since scattering in mmWave induces more than 20 dB attenuation (Shaham et al., 2018). In addition, the energy of the non-line-of-sight (NLoS) component is far less than that of the LoS component in mmWave communications, and the performance penalty caused by the consideration that only the LoS component exists is ignorable (Garcia et al., 2016). Moreover, the measurements have shown that paths are sparse in the geometric domain and are less likely to overlap, so we can assume that only one path lies in the main beam direction while other paths fall into the sidelobes. Additionally, there is severe path loss of mmWave propagation since vehicles are moving fast, which means that only the LoS components can provide the reliability for the high transmission rate in mmWave communications, while the NLoS components are negligible. Thus, we assume, without loss of generality, that the speed of users hardly changes within the BS coverage time period, and that the vehicles are moving uniformly with unknown speed and direction of heading.

### 2.2 Channel acquisition model

In this study, a novel system structure is introduced. Downlink multi-user MIMO communication with the BS employs a uniform linear array (ULA) with $N$ elements and $K$ users with a single receive antenna. By introducing DLA to reduce the number of required RF chains, the system model of mmWave massive MIMO can be expressed by

$$\boldsymbol{y}=\boldsymbol{H}^{\mathrm{H}}\boldsymbol{F}\boldsymbol{s}+\boldsymbol{n}, \tag{1}$$

where $\boldsymbol{H}=[\boldsymbol{h}_1,\boldsymbol{h}_2,\ldots,\boldsymbol{h}_k]\in\mathbb{C}^{N\times K}$ denotes the mmWave channel matrix between the BS and the MS, and $\boldsymbol{h}_i\in\mathbb{C}^{N\times 1}$ $(i=1,2,\ldots,k)$ is the beamspace channel of the $i^{\mathrm{th}}$ user. $\boldsymbol{s}\in\mathbb{C}^{K\times 1}$ is the original signal vector for all $K$ users with normalized power, and $\mathbb{E}(\boldsymbol{s}\boldsymbol{s}^{\mathrm{H}})=\boldsymbol{I}_K$. $\boldsymbol{F}\in\mathbb{C}^{N\times K}$ is the corresponding dimension-reduced digital precoding matrix satisfying $\mathrm{tr}(\boldsymbol{F}\boldsymbol{F}^{\mathrm{H}})\leq\delta$, where $\delta$ is downlink transmit power. $\boldsymbol{n}\sim\mathcal{CN}(0,\sigma^2\boldsymbol{I}_k)$ is the Gaussian noise with variance $\sigma^2$ corrupting the received signal. Let $\rho_k^{(l)}$ denote the $l^{\mathrm{th}}$ path gain from the ULA to the receive antenna of the $k^{\mathrm{th}}$ user, where $l=0$ corresponds to the LoS component and $l=1,2,\ldots,L$ represents $L$ NLoS components. Following the Saleh-Valenzuela channel model (Awad et al., 2015), we have

$$\boldsymbol{h}_k=\sqrt{\frac{N}{L+1}}\sum_{l=0}^{L}\rho_k^{(l)}\boldsymbol{a}(\psi_k^l), \tag{2}$$

where the array response vector corresponding to the $l^{\mathrm{th}}$ path is given by

$$\boldsymbol{a}(\psi_k^l)=\frac{1}{\sqrt{N}}\exp(-\mathrm{j}2\pi\psi_k^l i)_{i\in\mathcal{I}(N)}, \tag{3}$$

where $\psi_k^l=\frac{d}{\lambda}\sin\theta_k^{(l)}$ is defined as the spatial direction of the $l^{\mathrm{th}}$ component at the $k^{\mathrm{th}}$ user; $\lambda$ and $d$ are the signal wavelength and antenna spacing, respectively, usually satisfying $d=\lambda/2$; $\theta_k^{(l)}$ is the physical direction which is considered uniformly distributed in the interval $[-\frac{\pi}{2},\frac{\pi}{2}]$. $\mathcal{I}(N)$ is an index set, given by $\mathcal{I}(N)=\{m-(N-1)/2,m=0,1,\ldots,N-1\}$.

According to the previous analysis, the number of dominant scatters in mmWave fast time-varying channels is limited. It is a reasonable assumption that the LoS component is considered as the target path for the channel estimation, while the NLoS paths are ignorable. This assumption is even more true as the number of antennas increases and the beam width grows narrower (Shaham et al., 2018). Therefore, we consider the mmWave fast time-varying channel with only the LoS component, and Eq. (2) can be rewritten as

$$\boldsymbol{h}_k = \rho_k \boldsymbol{a}(\psi_k), \tag{4}$$

where the superscript $l$ is omitted for simplification.

As the mmWave signals are quasi-optical, the number of effective prorogation paths in mmWave communications is very limited, occupying only a small number of beams, which shows that the mmWave channel is sparse. To reduce the dimension of the MIMO systems and the number of required RF chains, DLA can be exploited to select a small number of dominant beams based on the sparsity of a mmWave channel. Such a DLA plays the role of a spatial discrete Fourier transform (DFT) matrix $\boldsymbol{U} \in \mathbb{C}^{N\times N}$, which can transform the conventional spatial domain into the beamspace channel at the transmitter (Gao et al., 2017a). $\boldsymbol{U}$ contains the array steering vectors of $N$ orthogonal directions (beams) covering the entire space as

$$\boldsymbol{U} = \left[\boldsymbol{a}(\overline{\psi}_1), \boldsymbol{a}(\overline{\psi}_2), \ldots, \boldsymbol{a}(\overline{\psi}_N)\right]^{\mathrm{H}}, \tag{5}$$

where $\overline{\psi}_n = \frac{1}{N}(n - \frac{N+1}{2})$ for $n$=$1, 2, \ldots, N$ are the spatial directions predefined by DLA. Then, the mmWave beamspace massive MIMO system can be presented by

$$\boldsymbol{y} = \boldsymbol{H}_b^{\mathrm{H}} \boldsymbol{F}_b \boldsymbol{s} + \boldsymbol{n}, \tag{6}$$

where $\boldsymbol{H}_b = \boldsymbol{U}^{\mathrm{H}}\boldsymbol{H} \in \mathbb{C}^{N\times K}$ is the beamspace channel with dimension $b$, and $\boldsymbol{F}_b = \boldsymbol{U}^{\mathrm{H}}\boldsymbol{F} \in \mathbb{C}^{N\times K}$ is the corresponding dimension-reduced digital precoding matrix with dimension $b$. The number of significant entries in each $\boldsymbol{h}_{b,k} = \boldsymbol{U}^{\mathrm{H}}\boldsymbol{h}_k$ $(k = 1, 2, \ldots, K)$ is considerably smaller than $N$, which represents the sparsity nature of the mmWave channel. Since each beam in the beamspace channel (i.e., $\boldsymbol{H}_b$) needs a dedicated RF chain, a few beams are selected from elements, which can reduce the dimension of the MIMO system and the number of required RF chains. In addition, due to the limited number of dominant scatterers in the mmWave prorogation environments, the beamspace channel has a sparse structure (Kabaoglu, 2009; Ma et al., 2018; Shaham et al., 2018). Thus, as shown in Fig. 2, we can select only a small number of appropriate beams according to the sparse beamspace channel to reduce the dimension of the MIMO system without significant performance loss:

$$\widetilde{\boldsymbol{y}} = \widetilde{\boldsymbol{H}}_b^{\mathrm{H}} \widetilde{\boldsymbol{F}}_b \boldsymbol{n} + \boldsymbol{n}, \tag{7}$$

where $\widetilde{\boldsymbol{H}}_b = \boldsymbol{H}_b(a, :)_{a\in\mathcal{A}}$ with $\mathcal{A}$ denoting the sparsity mask (Brady et al., 2013) is the effective channel matrix with dimension $b$ after beam selection, and $\widetilde{\boldsymbol{F}}_b \in \mathbb{C}^{K\times K}$ is the dimension-reduced digital precoding matrix with dimension $b$ after beam selection. Since the dimension of $\widetilde{\boldsymbol{F}}_b$ in Eq. (7) is much lower than that of $\boldsymbol{F}$ in Eq. (1), the beamspace channel can significantly reduce the number of required RF chains. In addition, the smallest number of required RF chains should be $N_{\mathrm{RF}} = K$ to guarantee the spatial multiplexing gains of $K$ users. Therefore, we consider $N_{\mathrm{RF}} = K$ without the loss of generality in the proposed scheme.

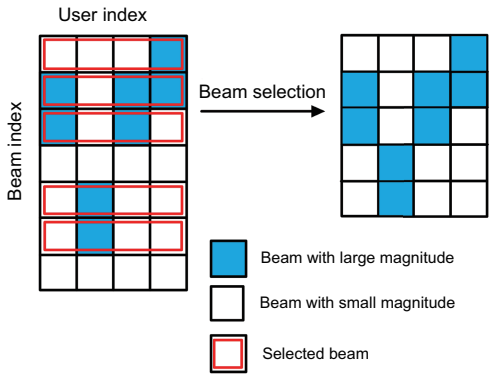


**Fig. 2 Illustration of the beam selection**

Next, we need to select only $K$ LoS paths to obtain a complete channel, which is equivalent to estimating $K$ beams. However, since the fast variation of mmWave beamspace channels is caused by user mobility, beam selection requires the BS to obtain the accurate channel state information (CSI) of the beamspace channel with a high dimension. In particular, conventional real-time channel estimation schemes involve unaffordable large pilot overhead (Brighente et al., 2020). For this purpose, a more efficient channel estimation scheme is designed in practical fast time-varying mmWave vehicle systems.

## 3 Proposed channel estimation algorithm

In the V2I scenario, the benefit of using position side information for mmWave beam alignment will be even greater. Generally, infrastructures locate at the side of a highway, which provides a wider angular region for searching the best beam. However, the NLoS path gain is less than the LoS path gain, and the number of effective paths is limited, which shows that LoS communication between the BS and the mobile user can be used to effectively improve the communication quality for mmWave fast time-varying channels. Therefore, it is reasonable to assume that the LoS path is a dominant component, while the NLoS paths can be ignored for mmWave V2I fast time-varying vehicular communication on a highway. Based on the above theoretical analysis, a novel time-varying channel estimation scheme is proposed (Fig. 1), which can significantly reduce the duration of channel estimation, making it a viable algorithm for the mmWave V2I fast time-varying communication scenario.

### 3.1 Analysis of the temporal variation law of the physical direction of the moving user in V2I scenarios

Inspired by the principle of Zhou et al. (1999) and the theoretical analysis in Section 2, a mathematical model of the trajectory of mobile users is established, as illustrated in Fig. 3. Since the vehicles are fast moving, the $k^{\text{th}}$ user's trajectory is considered as an approximate straight line with a constant speed in every time slot interval. Thus, we collect only the motion state in the $t^{\text{th}}$ time slot for channel estimation without loss of generality. Specifically, the channel information of the following time slots can be estimated by exploiting the motion state in the first three time slots, and the temporal variation law of physical direction is derived. This scheme can be directly applied to other users in the same way. In addition, it can be seen from Eqs. (3)–(5) that the physical direction $\theta_k$ (or the spatial direction $\psi_k$ in Eq. (3)) of the LoS component is a crucial parameter for determining the time-varying beamspace channel $\boldsymbol{h}_k$. Hence, to obtain $\boldsymbol{h}_k$, we need to be aware of the time-varying rule of physical direction $\theta_k(t)$.

To derive the temporal variation law of physical direction, a linear user motion model is considered as shown in Fig. 3, which is the geometrical relationship between the BS and the $k^{\text{th}}$ mobile user, and the directions parallel and vertical to the BS are defined as the $x$ and $y$ axes, respectively. The BS is set as the origin of the Cartesian coordinate system, which is equipped with DLA to simultaneously serve $K$ signal-antenna users, where a user moves from point $P$ to point $Q$ across different time slots. Since the channel is fast time-varying, it is a reasonable assumption that we consider only the trajectory of the $k^{\text{th}}$ user from point $U$ to point $W$ for channel estimation. Moreover, $\nu_k$ and $\alpha_k$ are the motion speed and motion direction of the $k^{\text{th}}$ user in time slot interval $T$, respectively, where $\nu_k$ and $\alpha_k$ are unknown but not time-varying. Additionally, the physical direction of the $k^{\text{th}}$ user in the $t^{\text{th}}$ time slot is denoted by $\theta_k(t)$, where $\theta_k(t)$ (i.e., DOA) is defined negative when the user is located on the left side of the origin $O$, i.e., $\theta_k(t) < 0$; otherwise, $\theta_k(t) > 0$. Because of the high speed of each user, each user moves linearly and uniformly, rather than time-varying in a time slot interval. Finally, $U$, $V$, and $W$ are the points of the $k^{\text{th}}$ mobile user in time slots $t$, $t+1$, $t+2$, respectively; $d_k(t)$, $d_k(t+1)$, …, $d_k(t+N)$ are the communication distances between the BS and the $k^{\text{th}}$ mobile user at the corresponding time slot.

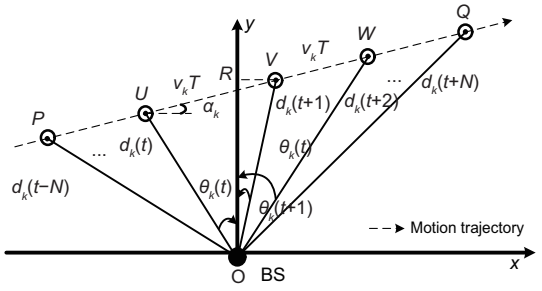


**Fig. 3 Location relationship model between the base station (BS) and the movement trajectory of the $k^{\text{th}}$ mobile user**

Our target is to predict $\theta_k(t+1)$ using $\theta_k(1)$, $\theta_k(2)$, …, $\theta_k(t)$. For far-field users, the following state vector is defined to describe the motion state of the $k^{\text{th}}$ target in time slot $t$:

$$\boldsymbol{f}_k(t) = [\theta_k(t), \upsilon_k(t), \alpha_k]^{\mathrm{T}}, \tag{8}$$

where the angular speed $\upsilon_k(t) = \frac{\nu_k}{d_k(t)}$ is defined as an auxiliary parameter. Then, the temporal variation law of the physical direction of each mobile user is derived by exploiting the geometrical relationship in

Fig. 3, namely, the correlation between the user's moving positions in adjacent time slots. Detailed process is as follows:

First, we focus on the physical direction $\theta_k(t)$. According to the right triangle $ROV$ in Fig. 3 and the tangent function, we can obtain

$$\begin{aligned}\tan\big(\theta_k(t+1)\big) &= \frac{|RV|}{|OR|}\\ &= \frac{\sin\big(\theta_k(t)\big)+\upsilon_k(t)T\cos\alpha_k}{\cos\big(\theta_k(t)\big)+\upsilon_k(t)T\sin\alpha_k},\end{aligned} \tag{9}$$

where $\sin\big(\theta_k(t)\big)<0$ and $\cos\alpha_k>0$. From Eq. (9) we have

$$\theta_k(t+1)=\arctan\left(\frac{\sin\big(\theta_k(t)\big)+\upsilon_k(t)T\cos\alpha_k}{\cos\big(\theta_k(t)\big)+\upsilon_k(t)T\sin\alpha_k}\right). \tag{10}$$

Then, we take the triangle $UOV$ into account, where $\theta_k(t)<0$, $\theta_k(t+1)>0$, and the cosine of $\angle OUV$ is calculated by exploiting the cosine rule:

$$\begin{aligned}\cos\angle OUV &= \frac{|UO|^2+|UV|^2-|OV|^2}{2\,|UO|\,|UV|}\\ &= \frac{|d_k(t)|^2+|\nu_kT|^2-|d_k(t+1)|^2}{2\,|d_k(t)|\,|\nu_kT|}.\end{aligned} \tag{11}$$

Then, by substituting $\upsilon_k(t)=\frac{\nu_k}{d_k(t)}$ into Eq. (11), Eq. (11) can be rewritten as

$$\begin{aligned}\sin\big[\theta_k(t)+\alpha_k\big] &= \frac{|d_k(t+1)|^2-|d_k(t)|^2-|\nu_kT|^2}{2\,|d_k(t)|\,|\nu_kT|}\\ &= \frac{\frac{|\upsilon_k(t)|^2}{|\upsilon_k(t+1)|^2}-1-|\upsilon_k(t)T|^2}{2|\upsilon_k(t)T|^2}.\end{aligned} \tag{12}$$

By simplifying Eq. (12), the angular speed $\upsilon_k(t+1)$ in time slot $t+1$ can be derived as

$$\upsilon_k(t+1)=\frac{\upsilon_k(t)}{\sqrt{1+2T\upsilon_k(t)\sin\big[\theta_k(t)+\alpha_k\big]+T^2\upsilon_k^2(t)}}. \tag{13}$$

Based on Eqs. (10) and (13) and the motion direction $\alpha_k$ as a constant value, the relationship between $\boldsymbol{f}_k(t\pm1)$ and $\boldsymbol{f}_k(t)$ can be written as

$$\boldsymbol{f}_k(t\pm1)=\boldsymbol{G}^{\pm}\big(\boldsymbol{f}_k(t)\big), \tag{14}$$

where $\boldsymbol{G}^{\pm}\big(\boldsymbol{f}_k(t)\big)$ is a function of $\boldsymbol{f}_k(t)$, and $\boldsymbol{G}^{\pm}\big(\boldsymbol{f}_k(t)\big)$ is given by

$$\boldsymbol{G}^{\pm}\big(\boldsymbol{f}_k(t)\big)=\begin{bmatrix}\arctan\left(\frac{\sin(\theta_k(t))\pm T\upsilon_k(t)\cos\alpha_k}{\cos(\theta_k(t))\pm T\upsilon_k(t)\sin\alpha_k}\right)\\ \frac{\upsilon_k(t)}{\sqrt{1\pm2T\upsilon_k(t)\sin[\theta_k(t)+\alpha_k]+T^2\upsilon_k^2(t)}}\\ \alpha_k\end{bmatrix}. \tag{15}$$

In addition, Eq. (14) can be applied recursively $N$ times to form the relationship between $\boldsymbol{f}_k(t\pm N)$ and $\boldsymbol{f}_k(t)$:

$$\begin{aligned}\boldsymbol{f}_k(t\pm N) &= \overbrace{\boldsymbol{G}^{\pm}\boldsymbol{G}^{\pm}\cdots\boldsymbol{G}^{\pm}}^{N}(\boldsymbol{f}_k(t))\\ &= \boldsymbol{G}^{\pm N}(\boldsymbol{f}_k(t)),\end{aligned} \tag{16}$$

where

$$\begin{aligned}&\boldsymbol{G}^{\pm N}(\boldsymbol{f}_k(t))\\ &=\begin{bmatrix}\arctan\left(\frac{\sin(\theta_k(t))\pm NT\upsilon_k(t)\cos\alpha_k}{\cos(\theta_k(t))\pm NT\upsilon_k(t)\sin\alpha_k}\right)\\ \frac{\upsilon_k(t)}{\sqrt{1\pm2NT\upsilon_k(t)\sin[\theta_k(t)+\alpha_k]+N^2T^2\upsilon_k^2(t)}}\\ \alpha_k\end{bmatrix}.\end{aligned} \tag{17}$$

Eq. (17) shows that once $\boldsymbol{f}_k(t)$ has been estimated, $\theta_k(t+N)$ can be predicted accordingly.

Next, we need to determine the location of the moving user in time slot $t$, and use the relationship in Eq. (14) between $\boldsymbol{f}_k(t+1)$ and $\boldsymbol{f}_k(t)$ to obtain the position of the next time slot. Thus, we use the physical direction $\theta_k(t)$ to reformulate $\upsilon_k(t)$ and $\alpha_k$ in $\boldsymbol{f}_k(t)$. Based on the triangle $UOV$ and the sine law, we can obtain

$$\frac{\nu_kT}{\sin[\theta_k(t+1)-\theta_k(t)]}=\frac{d_k(t+1)}{\sin[\frac{\pi}{2}-(-\theta_k(t))+\alpha_k]}. \tag{18}$$

The angular speed $\upsilon_k(t+1)$ is derived by decomposing Eq. (18) as

$$\upsilon_k(t+1)=\frac{\sin[\theta_k(t+1)-\theta_k(t)]}{T\cos[\theta_k(t)+\alpha_k]}. \tag{19}$$

Similarly, by exploiting the sine rule of

$$\frac{\nu_kT}{\sin[\theta_k(t+1)-\theta_k(t)]}=\frac{d_k(t)}{\sin[\frac{\pi}{2}-\theta_k(t+1)-\alpha_k]}, \tag{20}$$

we obtain

$$\upsilon_k(t)=\frac{\sin[\theta_k(t+1)-\theta_k(t)]}{T\cos[\theta_k(t+1)+\alpha_k]}. \tag{21}$$

In addition, by observing the triangle $UOW$, the following is available:

$$\frac{2\nu_kT}{\sin[\theta_k(t+2)-\theta_k(t)]}=\frac{d_k(t+2)}{\sin[\frac{\pi}{2}+\theta_k(t)+\alpha_k]}. \tag{22}$$

Eq. (22) can be decomposed and written as

$$\upsilon_k(t+2)=\frac{\sin[\theta_k(t+2)-\theta_k(t)]}{2T\cos[\theta_k(t)+\alpha_k]}. \tag{23}$$

Similarly, we can obtain

$$\frac{2\nu_k T}{\sin[\theta_k(t+2)-\theta_k(t)]}=\frac{d_k(t)}{\sin[\frac{\pi}{2}-\theta_k(t+2)-\alpha_k]}. \tag{24}$$

Furthermore, Eq. (24) can be expressed as

$$\upsilon_k(t)=\frac{\sin[\theta_k(t+2)-\theta_k(t)]}{2T\cos[\theta_k(t+2)+\alpha_k]}. \tag{25}$$

Based on Eqs. (18)–(25), the following observations can be achieved:

$$\upsilon_k(t+2)=\frac{\sin[\theta_k(t+2)-\theta_k(t)]}{2T\cos[\theta_k(t)+\alpha_k]}, \tag{26}$$

$$\alpha_k=\frac{2\eta_k\cos[\theta_k(t+2)]-\mu_k\cos[\theta_k(t+1)]}{2\eta_k\sin[\theta_k(t+2)]-\mu_k\sin[\theta_k(t+1)]}, \tag{27}$$

where $\eta_k=\sin[\theta_k(t+1)-\theta_k(t)]$ and $\mu_k=\sin[\theta_k(t+2)-\theta_k(t)]$.

By Eqs. (26) and (27) and the relationship $\boldsymbol{f}_k(t\pm1)=\boldsymbol{G}^{\pm}(\boldsymbol{f}_k(t))$ in Eq. (14), the physical direction $\theta_k(t+3)$ in the following $t+3$ time slots can be predicted in advance when the physical directions in time slots $t$, $t+1$, and $t+2$ have been separately estimated.

### 3.2 Characteristics of mmWave fast time-varying beamspace channels

To estimate the mmWave fast time-varying vehicle channels, we combine the time-varying physical direction with the characteristics of the mmWave time-varying beamspace channels to obtain the support of the time-varying channels (Gao et al., 2017a). Thus, we first need to know the characteristics of the time-varying beamspace channels. According to Eqs. (2)–(4), the time-varying beamspace channel $\widetilde{\boldsymbol{h}}_k$ of the $k^{\text{th}}$ user can be expressed as

$$\widetilde{\boldsymbol{h}}_k=\rho_k[\chi(\overline{\psi}_1-\psi_k),\chi(\overline{\psi}_2-\psi_k),\ldots,\chi(\overline{\psi}_N-\psi_k)]^{\mathrm{H}}, \tag{28}$$

where $\chi(x)=\frac{\sin(N\pi x)}{N\sin(\pi x)}$. Fig. 4 shows the normalized amplitude distribution of the elements in the time-varying channel.

From Fig. 4, we can observe that when the practical spatial direction $\psi_k$ in Eq. (3) exactly equals one of the predefined spatial directions $\overline{\psi}_n$ in Eq. (5), there is only one strongest element containing most of the power of $\widetilde{\boldsymbol{h}}_k$, which is the best case. Conversely, the worst case will happen when the distance between $\psi_k$ and one of the predefined spatial directions is equal to $1/(2N)$. Moreover, it was proved by

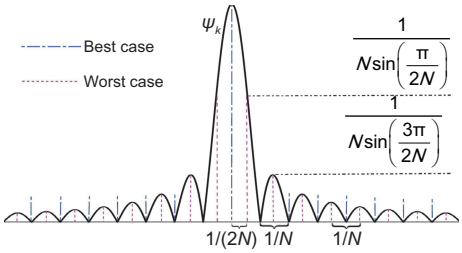


**Fig. 4 Normalized amplitude distribution of the elements in the time-varying channels**

Sayeed and Brady (2013) that by considering the channel with only the LoS component, the time-varying beamspace channel $\widetilde{\boldsymbol{h}}_k$ can be regarded as a sparse channel since most of the power of $\widetilde{\boldsymbol{h}}_k$ is focused on a small number of dominant elements, and the energy of other elements is negligible without obvious performance loss. Moreover, most of the power of $\widetilde{\boldsymbol{h}}_k$ is concentrated on one main peak, and other elements with weaker energy are uniformly located around it. From what we have discussed above, we can draw the conclusion that once the position of the strongest element of the time-varying channel $\widetilde{\boldsymbol{h}}_k(t)$ in time slot $t$ is determined, other stronger elements will uniformly locate around it. In other words, as long as the position of the main peak is estimated, the position of other elements of $\widetilde{\boldsymbol{h}}_k(t)$ in time slot $t$ can be obtained.

After that, the $M$ strongest elements of $\widetilde{\boldsymbol{h}}_k(t)$ can be obtained when the position $\widetilde{n}_k^*(t)$ of the strongest element of $\widetilde{\boldsymbol{h}}_k(t)$ is determined, while the other $M-1$ strongest elements will uniformly locate around it, where $M$ represents the sparsity of the channel and is defined as an even integer ($M$ can also be odd). There is only one strongest element that contains most of the power of $\widetilde{\boldsymbol{h}}_k(t)$ in time slot $t$ when the practical spatial direction $\psi_k(t)=\frac{d}{\lambda}\sin(\theta_k(t))$ is exactly equal to one of the predefined spatial directions $\overline{\psi}_n=\frac{1}{N}(n-\frac{N+1}{2})$ for $n=1,2,\ldots,N$, and the position $\widetilde{n}_k^*(t)$ of the strongest element of $\widetilde{\boldsymbol{h}}_k(t)$ can be achieved. Detailed proof can be found in Gao et al. (2017a), in Lemma 2.

Based on the conclusions derived above, the index $\widetilde{n}_k^*(t)$ of the strongest element of $\widetilde{\boldsymbol{h}}_k(t)$ is determined by $\psi_k(t)$ (or $\theta_k(t)$), and the relationship is as follows:

$$\begin{aligned}\widetilde{n}_k^*(t)&=\arg\min_{1\le n\le N}\left|\overline{\psi}_n(t)-\psi_k(t)\right|\\&=\arg\min_{1\le n\le N}\left|\overline{\psi}_n(t)-\frac{d}{\lambda}\sin(\theta_k(t))\right|.\end{aligned} \tag{29}$$

Thus, the position $\widetilde{n}_k^*(t)$ of the strongest element of channel $\widetilde{\boldsymbol{h}}_k(t)$ can be obtained by Eq. (29). However, since $\widetilde{\boldsymbol{h}}_k(t)$ is the time-varying channel, we need to reversely compute $\widetilde{n}_k^*(t)$ by Eq. (29) after predicting $\widetilde{\theta}_k(t)$ in Section 3.1. Furthermore, the support $\mathrm{supp}(\widetilde{\boldsymbol{h}}_k(t))$ of the sparse channel $\widetilde{\boldsymbol{h}}_k(t)$ can be uniquely determined by $\widetilde{n}_k^*$:

$$\mathrm{supp}(\widetilde{\boldsymbol{h}}_k(t)) = \mathrm{mod}_N(\widetilde{n}_k^*(t)-\frac{M}{2},\ldots,\widetilde{n}_k^*(t)+\frac{M-2}{2}), \quad (30)$$

where $\mathrm{mod}_N(\cdot)$ is the modulo calculation for $N$, which guarantees that all elements in $\mathrm{supp}(\widetilde{\boldsymbol{h}}_k(t))$ belong to $\{1,2,\ldots,N\}$. $\mathrm{Card}(\mathrm{supp}(\widetilde{\boldsymbol{h}}_k(t)))=M$, and $M$ determines how much power can be preserved by assuming that $\widetilde{\boldsymbol{h}}_k(t)$ is a sparse vector. From Eqs. (29) and (30), we can conclude that $\widetilde{n}_k^*(t)$ can be achieved when the physical direction $\theta_k(t)$ is obtained, and that $\mathrm{supp}(\widetilde{\boldsymbol{h}}_k(t))$ can be directly detected via Eq. (30).

### 3.3 Channel estimation scheme for mmWave fast time-varying vehicular channel

The movement of vehicles leads to the fast variation of mmWave beamspace channels, and the state vector of the process has evolved. Our aim is to obtain the LoS paths of the time-varying channel. The main idea of Algorithm 1 is that the estimated physical directions in the previous time slots are used to predict the physical direction in the following time slots. Then, the special sparse feature of the mmWave fast time-varying vehicular channel and the physical directions that have been derived to determine the PI of the channel are combined to estimate the complete time-varying channel. In the following, we will explain Algorithm 1 in detail:

The proposed algorithm is divided into two parts. The first part is to estimate the time-varying channel $\widetilde{\boldsymbol{h}}_k(t)$ using the conventional SD-based channel in the previous three time slots in step 2. Then in step 3, the position $n_k^*(t)$ of the strongest element of the channel is used to solve the predefined spatial direction $\overline{\psi}_{n_k^*(t)}=[n_k^*(t)-\frac{N+1}{2}]\frac{1}{N}$ in Eq. (5). Furthermore, according to the property in Eq. (29) that the actual space direction is approximately equal to the predefined space direction that is received, we have

$$\psi_k(t)\approx\overline{\psi}_{n_k^*(t)}. \quad (31)$$

**Algorithm 1** PI-based channel estimation algorithm

// Part 1: regular channel estimation
1: **for** $1\le t\le 3$ **do**
2: Estimate channel $\widetilde{\boldsymbol{h}}_k(t)$ by SD-based channel estimation
3: Obtain the position of the strongest element $n_k^*(t)$ based on the estimated channel
4: Detect the physical direction $\bar{\theta}_k(t)$ according to the position of the strongest element
5: **end for**
// Part 2: the proposed channel estimation
6: **for** $t>3$ **do**
7: Estimate the motion state $\boldsymbol{f}_k(t-1)=[\overline{\theta}_k(t-1),\overline{v}_k(t-1),\overline{\alpha}_k]^{\mathrm{T}}$
8: Predict the physical direction $\widetilde{\theta}_k(t)$
9: Reversely compute the position of the strongest element based on the predicted physical direction $\widetilde{\theta}_k(t)$
10: Obtain the PI of $\widetilde{\boldsymbol{h}}_k(t)$ based on $\widetilde{\theta}_k(t)$
11: Estimate the nonzero elements of $\widetilde{\boldsymbol{h}}_k(t)$ by the LS algorithm
12: Form the estimated channel $\widetilde{\boldsymbol{h}}_k^{\mathrm{e}}(t)$
13: Refine the physical direction $\overline{\theta}_k(t)$ according to the position of the strongest element
14: **end for**

Next, substitute $\psi_k(t)=\frac{d}{\lambda}\sin(\theta_k(t))$ and $\overline{\psi}_{n_k^*(t)}=(n_k^*(t)-\frac{N+1}{2})\frac{1}{N}$ into Eq. (31); then, Eq. (31) can be written as

$$\frac{d}{\lambda}\sin(\theta_k(t))\approx\left[n_k^*(t)-\frac{N+1}{2}\right]\frac{1}{N}. \quad (32)$$

Furthermore, in step 4, the time-varying physical direction can be represented as

$$\overline{\theta}_k(t)\approx\arcsin\left[\frac{\lambda}{dN}\left(n_k^*(t)-\frac{N+1}{2}\right)\right]. \quad (33)$$

Part 2 exploits $\overline{\theta}_k(t)$ in Eq. (33) and $\boldsymbol{f}_k(t\pm1)=\boldsymbol{G}^{\pm}(\boldsymbol{f}_k(t))$ in Eq. (14) to estimate the physical directions $\theta_k(t-3)$, $\theta_k(t-2)$, and $\theta_k(t-1)$ in the previous three time slots. Then in steps 7 and 8, the time-varying physical direction $\widetilde{\theta}_k(t)$ in the following time slot can be predicted by Eqs. (26) and (27). In step 10, $\widetilde{\theta}_k(t)$ and Eq. (29) are combined to detect the support $\mathrm{supp}(\widetilde{\boldsymbol{h}}_k(t))$ of the sparse channel $\widetilde{\boldsymbol{h}}_k(t)$ in Eq. (30). Finally, the channel estimation can be executed. However, it is worth noting that due to that $\widetilde{\boldsymbol{h}}_k(t)$ is a time-varying channel, we need to reversely compute the position of the strongest element of $\widetilde{\boldsymbol{h}}_k(t)$ in time slot $t$ using Eq. (29) in step

9. Thus, based on the predicted $\widetilde{\theta}_k(t)$, the position $\widetilde{n}_k^*(t)$ of the strongest elements of $\widetilde{\boldsymbol{h}}_k(t)$ is reversely calculated using Eq. (29), and the support of $\widetilde{\boldsymbol{h}}_k(t)$ is detected using Eq. (30) in step 10. Next, we can solve the support by substituting $\widetilde{n}_k^*(t)$ into Eq. (30). According to $\mathrm{supp}(\widetilde{\boldsymbol{h}}_k(t))$, $K$ beams of $K$ LoS paths can be selected by an adaptive selection network, which can reduce the dimension of the MIMO systems and the number of required RF chains. Finally, the LS algorithm is used to estimate $K$ corresponding nonzero elements and form the time-varying estimated channel $\widetilde{\boldsymbol{h}}_k^{\mathrm{e}}(t)$ in steps 11 and 12.

After $\widetilde{\boldsymbol{h}}_k(t)$ has been estimated, $\overline{\theta}_k(t)$ in Eq. (33) is further refined by $\widetilde{n}_k^*(t)$. The main reason is that the residual caused by the approximation in Eq. (31) when the physical direction $\widetilde{\theta}_k(t)$ is solved can be avoided by our algorithm. Moreover, both the speed $v_k(t)$ and the movement direction $\alpha_k$ of users are time-varying parameters with respect to $\theta_k(t)$ in Eqs. (26) and (27), respectively. In addition, the deviation induced by predicting $\widetilde{\theta}_k(t)$ in step 8 can be adaptively adjusted when $\alpha_k$ or $v_k(t)$ changes in step 13, until the estimated value is close to the actual one. Compared with the traditional scheme, the proposed scheme is suitable for the nonlinear mobile user scenario with time-varying channels, which can significantly improve the channel estimation accuracy.

## 4 Simulation results

In this section, we evaluate the performance of our proposed method. We consider a time-varying mmWave massive MIMO V2I system, where the BS is equipped with a 256-element DLA, and the number of RF chains is set to 3 to simultaneously serve $K = 3$ users. For each user in each time slot, the beamspace channel is regarded as a sparse vector with sparsity $M = 16$, and we assume that complex channel gain follows $\mathcal{CN}(0, 1)$. We totally observe 40 time slots with the time slot interval $T = 1$. The motion states of users 1–3 in the initial time slot 1 are set as $\boldsymbol{f}_1(1) = [\pi/11, 0.0154, 3\pi/4]^{\mathrm{T}}$, $\boldsymbol{f}_2(1) = [-\pi/10, 0.0071, \pi/6]^{\mathrm{T}}$, $\boldsymbol{f}_3(1) = [-2\pi/11, 0.014, 0]^{\mathrm{T}}$.

In Fig. 5, the physical direction estimation accuracy of the proposed channel scheme is evaluated in different time slots, where SNR is set as 10 dB. In the first three time slots, the conventional real-time SD-based estimation scheme in Gao et al. (2017a) is adopted to estimate the beamspace channel with $Q = 128$ pilots per time slot. After that, part 2 of Algorithm 1 is used to estimate the time-varying channel with $Q = 16$ pilots per time slot. From Fig. 5, we can see that the DOAs of three mobile users are estimated by the proposed algorithm with low pilot overhead, where the deviation between the estimated path and the true path is negligible, even for user 3 who moves nonlinearly with a time-varying moving speed.

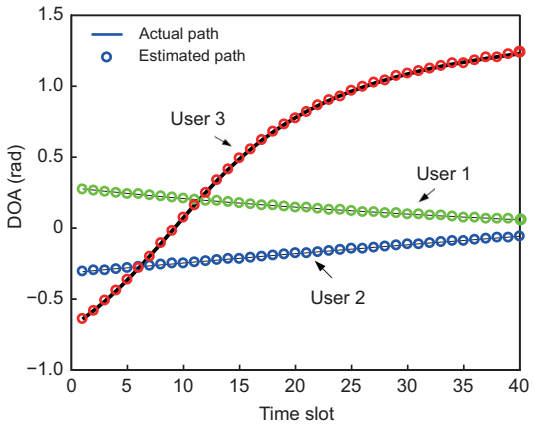


**Fig. 5 Direction-of-arrival (DOA) estimation performance of our method with SNR=10 dB and $Q = 16$**

Fig. 6 illustrates the normalized mean square error (NMSE) performance comparison of the channel estimation against SNR when we set $Q = 16$ pilots per time slot for both of the schemes; the SD-based channel estimation method is used for performance comparison. The NMSE is calculated as

$$\mathrm{NMSE} = \frac{\left\|\hat{\boldsymbol{h}}_k - \boldsymbol{h}_k\right\|^2}{||\boldsymbol{h}_k||^2}, \tag{34}$$

where $\hat{\boldsymbol{h}}_k$ denotes the estimated value of the channel $\boldsymbol{h}_k$. From Fig. 6, it can be observed that the proposed method outperforms the SD-based estimation technique. By comparison, the gap between these two schemes increases as the SNR increases. Obviously, the estimation accuracy of our scheme has been significantly improved under different SNR levels. This can be explained because the users' mobility usually causes the fast variation of the mmWave beamspace channel, and mmWave signals usually suffer from serious free-space path loss, which results in most of the elements of the channel having weak power. By contrast, our proposed method needs to estimate only the position of the strongest element. Using the

characteristics of the mmWave time-varying channel, the support of channel can be directly obtained with reliable performance, while the traditional scheme is suitable only for real-time channels with high pilot overhead. Therefore, the simulation results are consistent with our previous theoretical analysis.

Fig. 7 shows the NMSE performance comparison against the total number of instants $Q$, where SNR is set to 10 dB. Fig. 7 shows that, to achieve the same accuracy, the total number of instants $Q$ required by the proposed algorithm is much smaller than that of the SD-based scheme. For example, to achieve the NMSE of $6 \times 10^{-2}$, the total number of instants required by the SD-based channel estimation is about 110, whereas our scheme requires only 25 instants. Thus, we can conclude that our algorithm can efficiently estimate the time-varying channels with low pilot overhead.

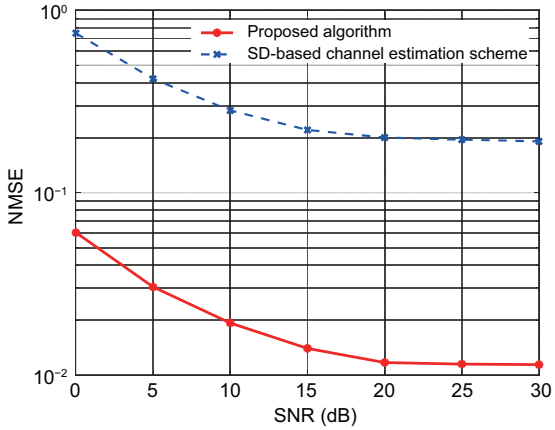


**Fig. 6 Normalized mean square error (NMSE) comparison between the SD-based channel estimation and the proposed scheme**

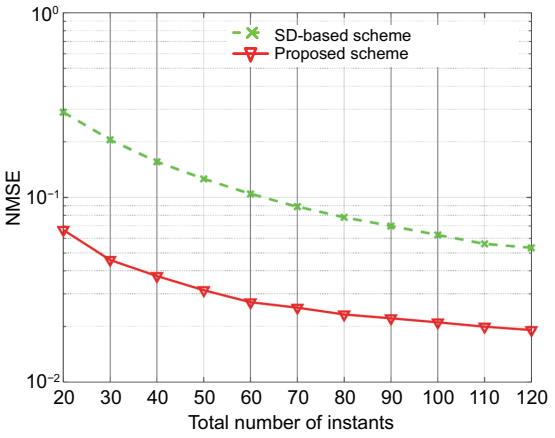


**Fig. 7 Normalized mean square error (NMSE) performance comparison against the total number of instants $Q$ for pilot transmission**

Finally, we compare the sum-rate performance of the maximization of capacity (MC) beam selection with different channels and show the results in Fig. 8, where we set SNR = 10 dB and $Q = 16$ pilots per time slot, and use the performance of the fully digital zero forcing (ZF) precoder using all beams with a perfect channel as the benchmark for comparison. Using our scheme, the sum-rate performance of the MC beam selection requires only 16 RF chains, which is quite close to that of the fully digital ZF precoder using 256 RF chains with perfect channel. This indicates that our method is obviously superior to the SD-based scheme. On the contrary, since the weak energy signal is seriously disturbed by noise, MC beam selection with the conventional scheme suffers from severe performance loss. This occurs because the traditional real-time scheme cannot be affordable with large pilot overhead due to the fast time-varying channel caused by high-mobility vehicles, whereas our proposed scheme can overcome the influence of the time-varying channel and significantly improve the channel estimation accuracy, which is consistent with our previous theoretical analysis. Thus, our scheme is more appropriate for fast time-varying vehicular channels.

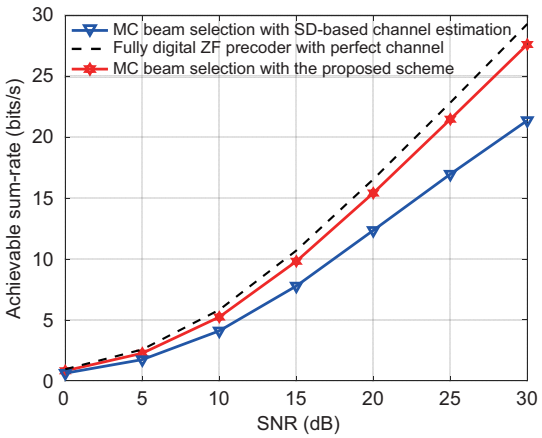


**Fig. 8 Sum-rate performance comparison between maximization of capacity beam selection with different channels**

## 5 Conclusions

In this study, we have investigated channel estimation in a fast-moving environment for mmWave

V2I communications. First, we have established the time-varying vehicle channel model, and focused on the structure of the system. Next, we have exploited the derived temporal variation law and the moving position vector of users in the time-varying channel to estimate the DOA of multiple mobile users. Finally, the complete time-varying channel has been estimated using the PI with low pilot overhead. Simulation results indicated that our scheme can significantly improve the channel estimation accuracy and exhibit superior performance under time-varying vehicle channel scenarios. Therefore, the proposed scheme in this paper is more suitable for mmWave fast time-varying vehicle systems.

## Contributors

Zhao YI designed the research. Zhao YI, Weixia ZOU, and Xuebin SUN processed the data. Zhao YI drafted the manuscript. Weixia ZOU and Xuebin SUN helped organize the manuscript. Zhao YI, Weixia ZOU, and Xuebin SUN revised and finalized the paper.

## Compliance with ethics guidelines

Zhao YI, Weixia ZOU, and Xuebin SUN declare that they have no conflict of interest.

## References

Awad MM, Seddik KG, Elezabi A, 2015. Channel estimation and tracking algorithms for harsh vehicle to vehicle environments. Proc IEEE 82nd Vehicular Technol Conf, p.1-5. https://doi.org/10.1109/VTCFall.2015.7390864

Bourdoux A, Cappelle H, Dejonghe A, 2011. Channel tracking for fast time-variant channels in IEEE802.11p systems. Proc IEEE Global Telecommunications Conf, p.1-6. https://doi.org/10.1109/GLOCOM.2011.6134024

Brady J, Behdad N, Sayeed AM, 2013. Beamspace MIMO for millimeter-wave communications: system architecture, modeling, analysis, and measurements. *IEEE Trans Antenn Propag*, 61(7):3814-3827. https://doi.org/10.1109/TAP.2013.2254442

Brighente A, Cerutti M, Nicoli M, et al., 2020. Estimation of wideband dynamic mmWave and THz channels for 5G systems and beyond. *IEEE J Sel Areas Commun*, 38(9):2026-2040. https://doi.org/10.1109/JSAC.2020.3000889

Choi J, Va V, Gonzalez-Prelcic N, et al., 2016. Millimeter-wave vehicular communication to support massive automotive sensing. *IEEE Commun Mag*, 54(12):160-167. https://doi.org/10.1109/MCOM.2016.1600071CM

Fernandez JA, Stancil D, Bai F, 2010. Dynamic channel equalization for IEEE 802.11p waveforms in the vehicle-to-vehicle channel. Proc 48th Annual Allerton Conf on Communication, Control, and Computing, p.542-551. https://doi.org/10.1109/ALLERTON.2010.5706954

Gao XY, Dai LL, Zhang Y, et al., 2017a. Fast channel tracking for terahertz beamspace massive MIMO systems. *IEEE Trans Veh Technol*, 66(7):5689-5696. https://doi.org/10.1109/TVT.2016.2614994

Gao XY, Dai LL, Han SF, et al., 2017b. Reliable beamspace channel estimation for millimeter-wave massive MIMO systems with lens antenna array. *IEEE Trans Wirel Commun*, 16(9):6010-6021. https://doi.org/10.1109/TWC.2017.2718502

Garcia N, Wymeersch H, Ström EG, et al., 2016. Location-aided mm-Wave channel estimation for vehicular communication. Proc IEEE 17th Int Workshop on Signal Processing Advances in Wireless Communications, p.1-5. https://doi.org/10.1109/SPAWC.2016.7536855

Gu YJ, Leshem A, 2012. Robust adaptive beamforming based on interference covariance matrix reconstruction and steering vector estimation. *IEEE Trans Signal Process*, 60(7):3881-3885. https://doi.org/10.1109/TSP.2012.2194289

Gu YJ, Goodman NA, Hong SH, et al., 2014. Robust adaptive beamforming based on interference covariance matrix sparse reconstruction. *Signal Process*, 96:375-381. https://doi.org/10.1016/j.sigpro.2013.10.009

Heath RW, Gonzãlez-Prelcic N, Rangan S, et al., 2016. An overview of signal processing techniques for millimeter wave MIMO systems. *IEEE J Sel Top Signal Process*, 10(3):436-453. https://doi.org/10.1109/JSTSP.2016.2523924

Kabaoglu N, 2009. Target tracking using particle filters with support vector regression. *IEEE Trans Veh Technol*, 58(5):2569-2573. https://doi.org/10.1109/TVT.2008.2005723

Kong LH, Khan MK, Wu F, et al., 2017. Millimeter-wave wireless communications for IoT-cloud supported autonomous vehicles: overview, design, and challenges. *IEEE Commun Mag*, 55(1):62-68. https://doi.org/10.1109/MCOM.2017.1600422CM

Ma X, Yang F, Liu SC, et al., 2018. Sparse channel estimation for MIMO-OFDM systems in high-mobility situations. *IEEE Trans Veh Technol*, 67(7):6113-6124. https://doi.org/10.1109/TVT.2018.2811368

Mehrabi M, Mohammadkarimi M, Ardakani M, et al., 2020. A deep learning based channel estimation for high mobility vehicular communications. Proc Int Conf on Computing, Networking and Communications, p.338-342. https://doi.org/10.1109/ICNC47757.2020.9049735

Palacios J, De Donno D, Widmer J, 2017. Tracking mm-Wave channel dynamics: fast beam training strategies under mobility. Proc IEEE Conf on Computer Communications, p.1-9. https://doi.org/10.1109/INFOCOM.2017.8056991

Rappaport TS, Xing YC, MacCartney GR, et al., 2017. Overview of millimeter wave communications for fifth-generation (5G) wireless networks—with a focus on propagation models. *IEEE Trans Antenn Propag*, 65(12):6213-6230. https://doi.org/10.1109/TAP.2017.2734243

Sayeed A, Brady J, 2013. Beamspace MIMO for high-dimensional multiuser communication at millimeter-wave frequencies. Proc IEEE Global Communications Conf, p.3679-3684. https://doi.org/10.1109/GLOCOM.2013.6831645

Shaham S, Ding M, Kokshoorn M, et al., 2018. Fast channel estimation and beam tracking for millimeter wave vehicular communications. https://arxiv.org/abs/1806.00161

Shen WQ, Dai LL, An JP, et al., 2019. Channel estimation for orthogonal time frequency space (OTFS) massive MIMO. *IEEE Trans Signal Process*, 67(16):4204-4217. https://doi.org/10.1109/TSP.2019.2919411

Wu XH, Zhu WP, Yan J, 2019. Channel estimation and tracking with nested sampling for fast-moving users in millimeter-wave communication. *Digit Signal Process*, 94:29-37. https://doi.org/10.1016/j.dsp.2019.05.009

Zhang C, Guo DN, Fan PY, 2016. Tracking angles of departure and arrival in a mobile millimeter wave channel. Proc IEEE Int Conf on Communications, p.1-6. https://doi.org/10.1109/ICC.2016.7510902

Zhou YF, Yip PC, Leung H, 1999. Tracking the direction-of-arrival of multiple moving targets by passive arrays: algorithm. *IEEE Trans Signal Process*, 47(10):2655-2666. https://doi.org/10.1109/78.790648